FEASIBILITY OF USING RICE STRAW ASH IN PORCELAIN TILE COMPOSITIONS

Álvaro Guzmán A (1*), Silvio Delvasto A (1), Vicente Amigó B (2), María Francisca Quereda V (3), Enrique Sánchez V (3)

(1) Grupo de Investigación de Materiales Compuestos, GMC. Escuela de Ingeniería de Materiales, Universidad del Valle, Cali, Colombia

(2) Instituto de Tecnología de Materiales, Universidad Politécnica de Valencia, Valencia, Spain

(3) Instituto de Tecnología Cerámica, Universidad Jaume I, Castellón, Spain

ABSTRACT

This paper presents the results of an investigation conducted on the feasibility of using rice straw ash (RSA) in porcelain tile compositions, partially or completely replacing the non-plastic raw materials (quartz and feldspar) that, together with the clays, constitute the major constituents of porcelain tile compositions. Using a triaxial mixture of these three materials, representative of those used in industrial practice in this type of composition, different compositions were formulated using of statistical mixture design of experiments, in which feldspar and feldspathic sand were replaced with different percentages of RSA, keeping the clay content constant in all formulations. Seventeen compositions were thus prepared according to a simplex-centroid mixture design. The mixtures were processed, reproducing industrial porcelain tile manufacturing conditions by the dry route: dry milling of the different components, dry mixing followed by powder wetting, forming by pressing, and fast firing at peak temperatures in the range 1140–1260 °C. Firing behaviour (linear shrinkage, water absorption, porosity, and bulk density) and the modulus of rupture of the fired pieces were evaluated as a function of the feldspar, feldspathic sand, and RSA contents in the mixtures.

The fired test pieces of all compositions, without and with the addition of RSA (M12, M8, M9, M13, and M6) in replacement of feldspar and quartz, exhibited the properties required for porcelain stoneware tile, group BIa (modulus of rupture > MPa 35 and water absorption ≤ 0,5%) according to the ISO 13006 standard. Additions of RSA in proportions of 15% and 50% in replacement of feldspar and quartz, respectively (M8), allowed porcelain tile to be fabricated that displayed no marked change in processing behaviour, in addition to obtaining a microstructure and the typical mineralogical phases of porcelain tile. However, the compositions in which RSA replaced feldspar and quartz in percentages of 100% (M6), and feldspar in a percentage of 100% (M13), required better control during the firing process, in addition to an increase in the optimum densification temperature to obtain key technical properties.

1. INTRODUCCION

Porcelain stoneware tile is a ceramic product characterised by low water absorption (< 0.5% according to the standard [1]), making it a high-performance material [2]. Porcelain tile is typically used in flooring, wall cladding, and ventilated façades [3]. In recent years, porcelain tile production and sales have grown, compared with production and sales rates of other ceramic construction materials, as a result of its high technological properties, particularly in regard to water absorption and frost resistance, and mechanical properties, such as modulus of rupture and abrasion resistance [2], [3], [4], [5].

A typical porcelain tile composition consists of 40–50% illitic–kaolinitic clay, 10–15% quartz, and 35 –45% feldspar (all percentages by weight) [6], [7]. Feldspar is a high-cost raw material and replacement would represent a significant reduction in porcelain tile production costs [8], [9]. Feldspar is a mineral flux commonly used in porcelain tile bodies. However, high-grade feldspathic minerals resources have recently begun to become scarce, thus making it necessary to consider alternative sources of fluxing materials that can form glassy phase at temperatures equal to or lower than those of the feldspars used at present [10]. To the above outlook is further to be added that deposits of good quality quartz sand in Colombia are limited. As a result, various alternative fluxes (soda-lime glasses, glass scrap (TV/PC cathode ray tubes and screens), blast furnace slag, metallurgical slags, zeolites, rice straw ash (RSA), etc.) and non-plastic materials (rice husk ash (RHA), silica fume (SF), fly ash (FA)) have been incorporated into porcelain tile body compositions, with a view to studying their effect on product firing behaviour and end-product technical properties [10-24]. However, the use of secondary raw materials is considered feasible only if the industrial process remains essentially unaltered and product quality and properties are not impaired [12], [16].

As feldspars generally come from just a few regions, e.g. Germany, Turkey, and France, in addition to the limited deposits of good quality quartz sands in Colombia, their possible replacement with rice straw ash (RSA) is an attractive option, taking into account the results of Guzmán et al. [21] and the K_2O and SiO_2 contained in RSA, which is of the order of 11.30–12.30% and 74.31-74.67% by weight of the ash, respectively [25], [26].

This study was undertaken to examine the feasibility of using rice straw ash (RSA) in ceramic mixtures to replace non-plastic materials (sodium feldspar and feldspathic sand) used in manufacturing porcelain tile bodies.

2. MATERIALS AND METHODS

2.1. MATERIALS

The raw materials used in preparing triaxial ceramic bodies were feldspathic sand, sodium feldspar, and illitic–kaolinitic clay. To obtain the RSA, the methodology described by Guzmán et al. [21] for the obtainment of RSA by Process D (calcination of the material to 800ºC to eliminate Cl and S as far as possible) was used. After the RSA had been obtained, it was subjected to milling for one hour in a laboratory ball mill. The chemical and mineralogical composition of the raw materials was determined by X-ray fluorescence (XRF) and X-ray diffraction (XRD), respectively (see Table I).

	Concentration by weight (%)			
Element and/or compound	Illitic–kaolinitic clay (A)	Sodium feldspar (F)	Feldspathic sand (AF)	RSA Process D (C)
SiO_2	59.00	70.00	91.00	79.62
Al_2O_3	27.30	18.00	5.00	0.27
Fe_2O_3	0.93	0.08	0.12	0.26
CaO	0.27	0.50	0.10	2.80
MgO	0.59	0.10	0.01	0.89
Na_2O	0.52	9.70	0.10	0.35
K_2O	2.45	0.35	2.50	10.53
TiO_2	1.45	0.11	0.08	-
MnO	< 0.01	-	-	0.71
P_2O_5	0.05	-	-	1.61
Cl	-	-	-	0.59
S	-	-	-	1.74
Zn	-	-	-	0.01
Rb	-	-	-	0.01
Sr	-	-	-	0.01
Cu	-	-	-	0.01
L.O.I.	7.29	0.50	1.10	0.59
Mineralogical phases	Kaolinite	Albite	Quartz	Cristobalite α
	Illite + M. Muscovite	Illite + M. Muscovite	Kaolinite	Tridymite α
	Quartz	Quartz	Orthoclase	
	Anatase	Others	Others	
	Albite			
	Others			

Table I. Chemical and composition mineralogical of the raw materials.

2.2. PROCESSING OF STD PORCELAIN TILE AND PORCELAIN TILE WITH RSA ADDITION

Different compositions were prepared for the test mixtures of ceramic powders, using the triaxial mixtures methodology. This methodology was introduced by Correia et al. [27] for use in traditional ceramic compositions, allowing systematic determination of the effect of each constituent and the possible interactions of the constituents on the properties of interest (bulk density, linear shrinkage, water absorption, apparent porosity, and modulus of rupture). Seventeen compositions were thus prepared according to a simplex-centroid mixture design. In this study, however, the results are described of the four most noteworthy compositions, together with those of the starting, STD mixture (M12).

With a view to obtaining the typical particle size of porcelain tile body compositions, the ceramic compositions were ground to a residue (R) of 1.5–2.0% on sieve » No. 325 (40 μm). **Table II** details the dry milling times required to prepare the formulations to a residue of 1.5–2.0% on a 40 μm sieve. One kg of each mixture was prepared.

MIXTURE	t (min)	% R (40 μm)
M9 (10AF.25F.25C.40A)	40	1.9
M12 (10AF.50F.0C.40A)	50	2.2
M13 (10AF.0F.50C.40A)	40	1.8
M6 (0AF.0F.60C.40A)	17	1.6
M8 (5AF.42.5F.12.5C.40A)	25	2.0

Table II. Milling time required to reach a residue of 1.5–2.0% on a 40 μm sieve.

To determine pressing and firing behaviour, cylindrical test pieces about 7 mm thick and 40 mm in diameter, in addition to prism-shaped test pieces measuring 80x20x6 mm, were prepared to determine the mechanical properties. The test pieces were formed at a moisture content of 5.5% (on a dry basis) by uniaxial pressing at a pressure of 400 kg/cm2. After they had been pressed, the test pieces were dried at 110 ± 5 °C in an electric laboratory oven. They were then sintered in a Pirometrol R electric laboratory kiln with a heating ramp of 70 °C/min between 25 °C and 500 °C, and 25 °C/min from 500 °C to the respective peak firing temperature. The residence time at peak firing temperature was 6 minutes, and the fired test pieces were cooled inside the kiln in order to avoid macroscopic residual stresses. The peak firing temperatures encompassed the range 1140–1260 °C, at intervals of 20°C, depending on each composition. The measurements of the dry and fired dimensions of the test pieces were made using a slide calliper.

The maximum densification temperature was determined for each mixture from the vitrification curve (see Figure 1), constructed after determining the bulk density, using the experimental conditions described previously.

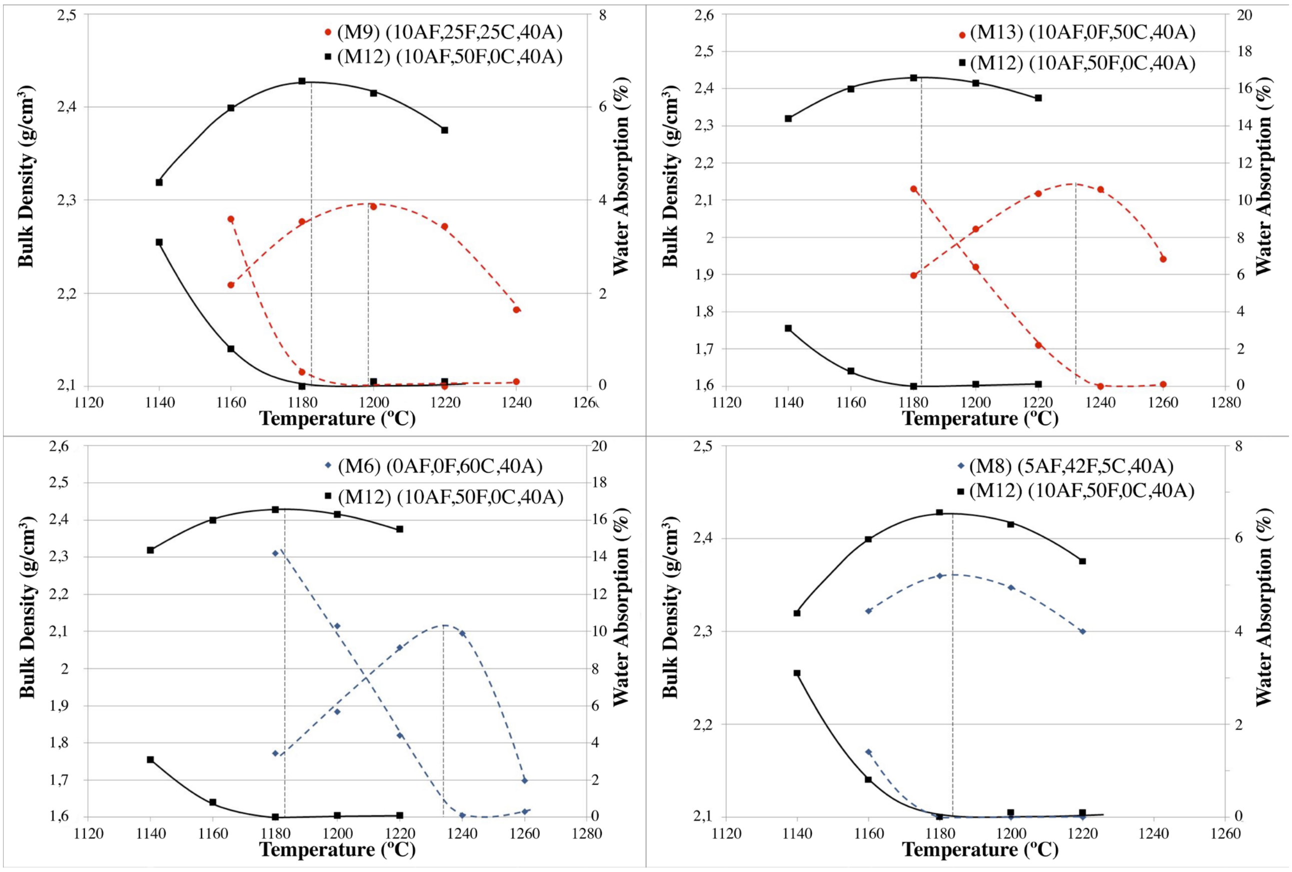

Figure 1. Bulk density of the fired porcelain tile test pieces M12, M9, M13, M6, and M8 as a function of firing temperature.

Owing to the scarce variation of water absorption with temperature at values below 1%, it was preferable to determine the maximum densification temperature as the characteristic temperature for industrial firing temperatures instead of the temperature at which the water absorption was less than 0.5%.

The technological properties of the fired test pieces were evaluated by performing the following tests: linear shrinkage, apparent porosity, water absorption, and bulk density according to standards ASTM C326-09, ASTM C329-88 (2011), and ASTM C373-88 (2006), in addition to the modulus of rupture, determined analogously to standard method ASTM C674-88 (2006) by means of a three-point bending test assembly, the span between supports being 62.2 mm and the load application rate being 5 mm/min. An average of ten measurements was taken for this purpose. In the STD mixture (M12) and the mixture with RSA in replacement of feldspar that exhibited the best modulus of rupture, the main crystalline phases was identified by XRD using a PANalytical X'Pert PRO X-ray diffractometer. The microstructural characteristics were observed by scanning electron microscopy (SEM), for which the fracture surface of each sample was polished and attacked with a hydrofluoric acid (HF) solution at 5% for 3 min, washed with distilled water and ethyl alcohol, and subsequently dried and coated with carbon.

3. RESULTS AND DISCUSSION

The chemical composition, determined by XRF, of the RSA obtained by process D showed that the main constituents were SiO_2 and K_2O (see **Table I**), corroborating the results reported by Jenkins et al. [25] and Thy et al. [26]. With relation to the clay, this consisted mainly of SiO_2 and Al_2O_3. In addition, it displayed low contents of K_2O and TiO_2 (2.5% and 1.5%, respectively), in which the K_2O could act as a flux, while TiO_2 was a chromophore oxide that provided a yellowish hue [28]. The feldspar, in turn, consisted mainly of SiO_2 and Al_2O_3, as well as 9.7% Na_2O, indicating that it was a sodium feldspar. On the other hand, the feldspathic sand mainly contained SiO_2 and Al_2O_3, in addition to 2.5% K_2O, which could act as a flux.

Feasibility of using RSA from process D as a flux in porcelain tile compositions

The replacement of feldspar and quartz with RSA in the mixture, in general, led to an increase in the SiO_2, K_2O, MgO, and CaO contents, in addition to a reduction in the Al_2O_3 and Na_2O contents (**Table III**).

Element and/ or compound	Concentration by weight (%)				
	M12	M8	M9	M13	M6
SiO_2	67.70	67.85	70.11	72.51	71.37
Al_2O_3	20.42	18.85	15.99	11.56	11.08
Fe_2O_3	0.42	0.44	0.47	0.51	0.53
CaO	0.37	0.68	0.94	1.52	1.79
MgO	0.29	0.39	0.48	0.68	0.77
Na_2O	5.07	4.38	2.73	0.39	0.42
K2O	1.41	2.57	3.95	6.50	7.30
TiO_2	0.64	0.63	0.62	0.59	0.58
MnO	0.00	0.09	0.18	0.36	0.43
P2O5	0.02	0.22	0.42	0.83	0.99
Cl	0.00	0.07	0.15	0.30	0.35
S	0.00	0.22	0.44	0.87	1.04
Zn	0.00	0.00	0.00	0.01	0.01
Rb	0.00	0.00	0.00	0.01	0.01
Sr	0.00	0.00	0.00	0.01	0.01
Cu	0.00	0.00	0.00	0.01	0.01
L.O.I.	3.28	3.26	3.30	3.32	3.27

Table III. Chemical composition of the mixtures (% by total weight).

Using the vitrification curves of the mixtures M12 (STD), M8, M9, M13, and M6 (see Figure 1), the optimum firing temperatures were determined to be 1183 °C, 1183 °C, 1199 °C, 1232 °C, 1234 °C, respectively.

The results of the technical properties obtained for each dry as well as fired composition, at its respective optimum firing temperature, are detailed in **Table IV**.

Technical properties	M12	M8	M9	M13	M6
Dry bulk density (g/cm^3)	1.91	1.83	1.79	1.72	1.65
Optimum firing temperature (°C)	1183	1183	1199	1232	1234
Linear shrinkage (%)	8.1	8.7	8.6	7.8	8.6
Fired bulk density (g/cm^3)	2.43	2.36	2.30	2.14	2.12
Water absorption (%)	<0.1	<0.1	<0.1	0.4	0.2
Apparent porosity (%)	<0.1	<0.1	<0.1	0.9	0.5
Modulus of rupture (MPa)	69	67	62	48	48

Table IV. Physical properties of the green and fired test pieces obtained at their optimum firing temperature.

The increase in the quantity of RSA in the mixture decreased test piece compactness, evidenced by a reduction in dry bulk density. This behaviour could stem from the fact that it adversely affected the balance between the non-plastic and the colloidal particles, raising the linear shrinkage of the fired test pieces. Compositions M8, M9, and M6 displayed this behaviour, with an increase in linear shrinkage in comparison with STD mixture M12 (8.1%). However, composition M13 exhibited a reduction in linear shrinkage, which could be related to its high quartz content (Table III).

The optimum vitrification range is obtained when the apparent porosity minimises, which tends to be close to zero, and bulk density and linear shrinkage simultaneously maximise. Firing above the vitrification range has a drastic adverse effect on the physical properties owing to an increase in the pressure of the gases trapped in the pores, producing swelling or bloating of the piece [5]. The maximum bulk density of each composition decreased as the replacement of feldspar and quartz with RSA increased, in comparison with that of STD mixture M12, as a result of the lower dry bulk density of the compositions with RSA. Mixture M8 exhibited the highest bulk density (2.36 g/cm^3) with respect to the other mixtures with RSA. Thus, mixtures M9, M13, and M6 displayed a reduction in bulk density (2.30 g/cm^3, 2.14 g/cm^3, and 2.12 g/cm^3, respectively) to the extent of being lower than the minimum value of 2.30 g/cm^3 in European standard UNI EN 87 [29].

The apparent porosity and water absorption percentage of mixtures M8 and M9 displayed similar trends to those of STD mixture M12. However, mixtures M13 and M6 exhibited higher values, which could be attributed to different factors, such as their low dry density and the bloating caused by the greater content in gas-generating substances

(Fe_2O_3, Cl, and PPI) in the RSA, in addition to the increase in the quantity of SiO_2, which reduced the sintering capacity, and the increase in the quantity of liquid phase of potassium origin, reducing its viscosity in comparison with that of the liquid phase of sodium origin [30]. These phenomena were corroborated by the decreased shrinkage and increased porosity displayed by mixtures M13 and M6 (see **Table IV**), typical behaviour in the bloating phenomenon during liquid-phase sintering of traditional ceramics [5].

The modulus of rupture of the fired test pieces (see **Table IV**) evidences a similar trend to that displayed by fired bulk density. The previous phenomena are consistent with Braganca and Bergmann [9], who noted that generally, at greater bulk density, the modulus of rupture increased.

According to the criteria of standard IS0 13006 for dry-pressed ceramic tiles, ceramic tile is defined as porcelain stoneware tile belonging to group BIa, when it exhibits a modulus of rupture > 35 MPa and water absorption 0.5%. In view of the results of the modulus of rupture and water absorption (see **Table IV**), compositions M12, M8, M9, M13, and M6 could all be deemed porcelain stoneware tile belonging to group BIa. However, in compositions M9, M13, and M6, there must also be an increase in the optimum firing temperature. In addition, in mixtures such as M13 and M6, the optimum firing range was very narrow (see **Figure 1**), reducing the feasibility of using these mixtures on an industrial scale.

The SEM micrographs at 100X in backscattered electron (BSE) mode of the polished surfaces (see Figure 2 (a and b)) showed that the surface of the test piece fired under maximum densification conditions of composition M8 displayed a greater quantity of closed pores than the test piece of composition M12; which was consistent with the density and porosity values noted previously.

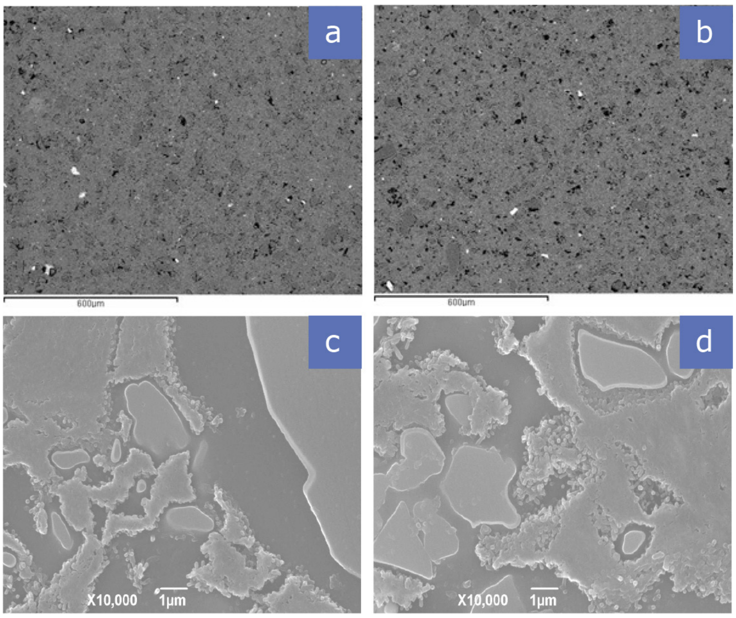

Figure 2. SEM micrographs in BSE mode of polished surfaces of fired test pieces M12 (a) and M8 (b) (100X); and SEM micrographs in SEI (secondary electron imaging) mode of polished surfaces of fired test pieces M12 (c) and M8 (d) (10000X).

The SEM micrographs at 10000X in secondary electron imaging (SEI) mode (see **Figure 2** (**c and d**)) show the presence of primary mullite crystals and quartz crystals embedded in a glassy phase in the microstructure of fired test pieces of compositions M12 and M8.

The SEM results were corroborated by XRD tests of fired test pieces of compositions M12 and M8 (see **Figure 3**), highlighting the presence of a-quartz (2θ= 20.86° and 26.64º) (ICSD 83849), albite (2θ= 22.03° and 27.91º) (ICSD 240519), and mullite (2θ= 16.43º; 33.21º; 35.26º; 39.24°, and 40.87º) (ICSD 99328), this last phase being partly responsible for porcelain mechanical strength. In addition, in the mixture to which RSA had been added (M8) the presence of a-cristobalite was evidenced (2θ= 21.76º) (ICSD 74530), basically stemming from the RSA.

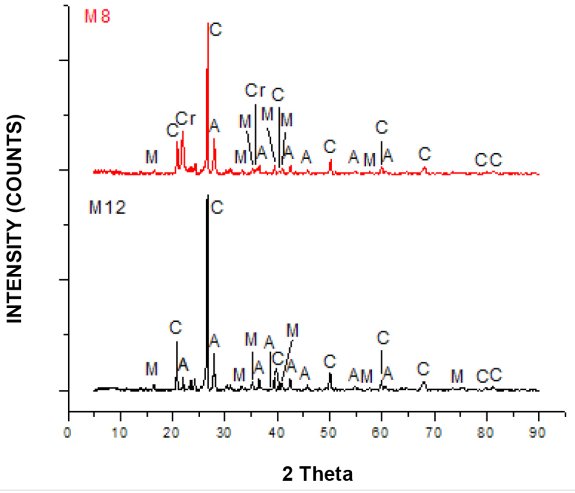

Figure 3. Crystalline phases present in fired test pieces of compositions M12 (a) and M8 (b) (M = mullite, C = quartz, Cr = cristobalite, A = albite).

4. CONCLUSIONS

The study shows that RSA displayed a non-plastic, fluxing character, allowing it to be used to partially replace feldspar and quartz in porcelain tile compositions. No pronounced change took place in the technological process when RSA was added to the composition in quantities of 15% and 50% in replacement of feldspar and quartz, respectively, allowing typical porcelain tile mineralogical phases and microstructure to be obtained.

The fired test pieces of all the compositions studied with an RSA addition (M8, M9, M13, and M6) exhibited the characteristics required of porcelain stoneware tile, BIa group (modulus of rupture > 35 MPa and water absorption ≤ 0.5%) according to standard ISO 13006. However, in those compositions in which RSA completely replaced quartz and feldspar (M6), or only completely replaced feldspar (M13), the optimum firing range was narrower, in addition to requiring higher firing temperatures. This reduced the feasibility of using these mixtures on an industrial scale.

5. ACKNOWLEDGEMENTS

The authors thank Universidad del Valle (Colombia), Instituto de Tecnología Cerámica (ITC), Instituto de Tecnología de Materiales de la Universidad Politécnica de Valencia, CENM, and COLCIENCIAS for the support provided to conduct this study. In particular, this paper presents the partial results of the research study "Rice Straw Ash-Based Triaxial Ceramics" code 110652128358 supported by COLCIENCIAS, Call 521 of 2010, contract RC. No. 325-2011.

REFERENCES

[1] Norma ISO 13006:1998. Ceramic tiles - Definitions, classification, characteristics and marking. International Organization for Standardization, 1998.

[2] Sánchez, E., Ibáñez, M.J., García-Ten, J., Quereda, M.F., Hutchings, I.M. y Xu, Y.M., 2006. Porcelain tile microstructure: Implications for polished tile properties. Journal of the European Ceramic Society., 26(13), pp. 2533-2540.

[3] Zanelli, C., Raimondo, M., Guarini, G. y Dondi, M., 2011. The vitreous phase of porcelain stoneware: Composition, evolution during sintering and physical properties. Journal of Non-Crystalline Solids., 357(16-17), pp. 3251–3260.

[4] De Noni Jr, A., Hotza, D., Cantavella, V. y Sánchez, E., 2008. Analysis of the development of microscopic residual stresses on quartz particles in porcelain tile. Journal of the European Ceramic Society., 28(14), pp. 2629–2637.

[5] Márquez, J.M., Rincón, J.M. y Romero, M., 2008. Effect of firing temperature on sintering of porcelain stoneware tiles. Ceramics International., 34(8), pp. 1867-1873.

[6] Andreola, F., Barbieri, L., Corradi, A., Lancellotti, I. y Manfredini, T., 2002. Utilisation of municipal incinerator grate slag for manufacturing porcelainized stoneware tiles manufacturing. Journal of the European Ceramic Society., 22(9–10), pp. 1457–1462.

[7] Zanelli, C., Raimondo, M., Dondi, M., Guarini. y Tenorio, P.M., 2004. Sintering mechanisms of porcelain stoneware tiles. In Qualicer 2004, Proceedings of the VIII World Congress on Ceramic Tile Quality, Cámara Oficial de Comercio, Industria y Navegación. Castellón, España, [pdf] papers C, pp. 247-259. Disponible a través de: <http://aulavirtual.camaracastellon.com/qualicerCD/pdf/0413191e.pdf>[Consultado 22 Enero 2011].

[8] Andreola, F.; Barbieri, L.; Karamanova, E.; Lancellotti, I. y Pelino, M., 2008. Recycling of CRT panel glass as fluxing agent in the porcelain stoneware tile production. Ceramics International., 34(5) 1289–1295.

[9] Braganca, S.R.; Bergmann, C.P., 2004. Traditional and glass powder porcelain: technical and microstructure analysis. Journal of the European Ceramic Society., 24(8) 2383–2388.

[10] Dana, K. y Das, S.K., 2004a. Partial substitution of feldspar by B.F slag in triaxial porcelain: Phase and microstructural evolution. Journal of the European Ceramic Society., 24(15-16) 3833–3839.

[11] Dana, K., Das, S. y Das, S.K., 2004b. Effect of substitution of fly ash for quartz in triaxial kaolin–quartz–feldspar system. Journal of the European Ceramic Society., 24(10-11), pp. 3169–3175.

[12] Matteucci, F., Dondi, M. y Guarini, G., 2002. Effect of soda-lime glass on sintering and technological properties of porcelain stoneware tiles. Ceramics International., 28(8), pp. 873-880.

[13] Dana, K. y Das, S.K., 2003. High strength ceramic floor tile compositions containing Indian metallurgical slags. Journal of Materials Science Letters., 22(5), pp. 387–389.

[14] Dana, K., Dey, J. y Das, S.K., 2005. Synergistic effect of fly ash and blast furnace slag on the mechanical strength of traditional porcelain tiles. Ceramics International., 31(1), pp. 147-152.

[15] Dana, K. y Das, S.K., 2008. Enhanced resistance to thermal cycling of slag-containing vitrified porcelain tiles. Industrial Ceramics., 28(2), pp. 121-124.

[16] Tucci, A., Esposito, L., Rastelli, E., Palmonari, C. y Rambaldi, E., 2004. Use of soda-lime scrap-glass as a fluxing agent in a porcelain stoneware tile mix. Journal of the European Ceramic Society., 24(1), pp. 83-92.

[17] De Gennaro, R., Cappelletti, P., Cerri, G., De Gennaro, M., Dondi, M., Guarini, G., Langella, A. y Naimo, D., 2003. Influence of zeolites on the sintering and technological properties of porcelain stoneware tiles. Journal of the European Ceramic Society., 23(13), pp. 2237–2245.

[18] De Gennaro, R., Dondi, M., Cappelletti, P., Cerri, G., De Gennaro, M., Guarini, G., Langella, A., Parlato, L. y Zanelli, C., 2007. Zeolite–feldspar epiclastic rocks as flux in ceramic tile manufacturing. Microporous and Mesoporous Materials., 105(3), pp. 273–278.

[19] Demirkiran, A.S., Artir, E. y Avci, E., 2008. Effect of natural zeolite addition on sintering kinetics of porcelain

bodies. Journal of Materials Processing Technology., 203(1-3), pp. 465-470.

[20] Raimondo, M., Zanelli, C., Matteucci, F., Guarini, G., Dondi, M. y Labrincha, J.A., 2007. Effect of waste glass (TV/PC cathodic tube and screen) on technological properties and sintering behaviour of porcelain stoneware tiles. Ceramics International., 33(4), pp. 615–623.

[21] Guzmán, A., Delvasto, S., Sánchez, E. y Amigó, V., 2013. Cenizas del tamo de arroz como substituto del feldespato en la fabricación de cerámica blanca. Boletín de la Sociedad Española de Cerámica y Vidrio., 52(1), pp. 25-30.

[22] Prasad, C.S., Maiti, K.N. y Venugopal, R., 2001. Effect of rice husk ash in whiteware compositions. Ceramics International., 27(6), pp. 629-635.

[23] Prasad, C.S., Maiti, K.N. y Venugopal, R., 2002. Effect of silica fume addition on the properties of whiteware compositions. Ceramics International., 28(1), pp. 9-15.

[24] Dana, K. y Das, S.K., 2004b. Evolution of microstructure in fly ash-containing porcelain body on heating at different temperatures. Bulletin of Materials Science, 27(2), pp. 183-188.

[25] Jenkins, B.M.; Baxter, L.L.; Miles Jr, T.R.; Miles, T.R., 1998. Combustion properties of biomass. Fuel Processing Technology., 54(1-3) 17-46.

[26] Thy, P.; Jenkins, B.M.; Grundvig, S.; Shiraki, R. y Lesher, C.E., 2006. High temperature elemental losses and mineralogical changes in common biomass ashes. Fuel., 85(5-6) 783-795.

[27] Correia, S.L., Oliveira, A.P.N., Hotza, D., Segadães, A.M., 2006. Properties of Triaxial Porcelain Bodies: Interpretation of Statistical Modeling. Journal of the American Ceramic Society., 89(11), p. 3356-3365.

[28] Barba, A., Beltrán, V., Felíu, C., García, J., Ginés, F., Sánchez, V.E., Sanz, V. Materias primas para la fabricación de soportes de baldosas cerámicas. 2da Edición. 2002. Castellón: Instituto de Tecnología Cerámica (ITC), p. 272-286.

[29] Biffi, G. O gres porcelanato: manual de fabricação e técnicas de emprego. 3.ed São Paulo: Faenza Editrice do Brasil Ltda, 2002.

[30] Das, S.K. y Dana, K., 2003. Differences in densification behaviour of K and Na-feldspar-containing porcelain bodies. Thermochimica Acta., 406(1-2), pp. 199-206.